Saudi Journal of Biological Sciences 28 (2021) 427–439

Contents lists available at ScienceDirect

Saudi Journal of Biological Sciences

journal homepage: www.sciencedirect.com

Original article

Psidium guajava Linn leaf ethanolic extract: In vivo giardicidal potential with ultrastructural damage, anti-inflammatory and antioxidant effects

Safaa I. Khedr [a,*], El Hassan M. Mokhamer [b], Amal A.A. Hassan [b], Asmaa S. El-Feki [b], Gihan M. Elkhodary [b], Mohamed S.A. El-Gerbed [b]

[a] Department of Medical Parasitology, Faculty of Medicine, Alexandria University, Alexandria, Egypt
[b] Department of Zoology, Faculty of Science, Damanhour University, Damanhour, Egypt

ARTICLE INFO

Article history:
Received 26 August 2020
Revised 17 October 2020
Accepted 18 October 2020
Available online 27 October 2020

Keywords:
Giardia lamblia
Psidium guajava leaf extract
Duodenal ultrastructure
Tumor necrosis factor-α
Nitric oxide
Superoxide dismutase

ABSTRACT

Introduction and aim: Considering the magnitude of giardiasis problem, the side-effects of the used anti-giardia drugs and the resistance posed against them, the current study aimed to evaluate the *in-vivo* giardicidal effect of *Psidium guajava* leaf extract (PGLE).

Methods: For fulfilling this aim, five Swiss-albino mice groups were included; GI: non-infected, GII: *Giardia*-infected and non-treated, GIII: *Giardia*-infected and metronidazole-treated, GIV: *Giardia*-infected and PGLE-treated, and GV: *Giardia*-infected and treated with both metronidazole and PGLE. Treatment efficacy was assessed via; *Giardia* cyst viability and trophozoite count, trophozoite electron microscopic ultrastructure, duodenal histopathological scoring, immunohistochemistry for TNF-α and duodenal scanning electron microscopy. Moreover, mice serum liver enzymes, total bilirubin, albumin, lipid profile including; total cholesterol, HDL, LDL and triglycerides were assessed. Additionally, hepatic oxidative stress markers including; malondialdehyde (MDA), nitric oxide (NO), reduced glutathione (GSH) and superoxide dismutase (SOD) were measured.

Results: Results showed that PGLE whether alone or combined with metronidazole has induced significant trophozoite count reduction and major architectural changes. Duodenal histological improvement, and local protective anti-inflammatory effect were confirmed. PGLE has also helped in healing of *Giardia*-induced gut atrophy. Thus, offered a comprehensive therapy for both the pathogen and the resultant pathological sequalae. Serum markers showed favorable hepatoprotective effect. Total cholesterol, LDL and triglycerides levels were less in PGLE-treated group than in metronidazole-treated group. Hepatic oxidative stress markers revealed the promising extract antioxidant effect. This study highlights, the promising *in-vivo* giardicidal PGLE activity, that was comparable to metronidazole, thus, the extract would be an ideal strongly recommended treatment for giardiasis. When combined with metronidazole, the extract potentiated its therapeutic effect. Besides, having hepatoprotective, anti-inflammatory, and antioxidant properties, the extract can combat the major side effects of metronidazole therapy.

1. Introduction

Giardia lamblia (*G. lamblia*) is an enteric protozoan that causes diarrhea. It infects up to ~28.2 million new cases every year, worldwide (Ryan et al., 2019). Owing to its magnitude, giardiasis was included by the WHO in the 'Neglected Disease Initiative' (Savioli et al., 2006; and Tian et al., 2010). Pathogenesis caused by *G. lamblia* is multifactorial, being, most importantly, mechanical and inflammatory, through trophozoite attachment to the host intestinal epithelium by the trophozoite ventral disc (Hanevik et al., 2007). Tumor necrosis factor-alpha (TNF-α) is a pro-inflammatory cytokine that plays a pivotal role in the initiation and continuation of inflammation process (Cabal-Hierro and Lazo, 2012). TNF-α contributes to protection against *G. lamblia* infection and determines the parasite burden (Zhou et al., 2007).

Abbreviations: G. lamblia, *Giardia lamblia*; PGLE, *Psidium guajava* Linn. leaf extract; MNZ, metronidazole; H&E, hematoxylin and eosin; SEM, scanning electron microscopy; TEM, transmission electron microscopy; TNF-α, tumor necrosis factor-alpha; AST, aspartate aminotransferase; ALT, alanine aminotransferase; LDL, low-density lipoproteins; HDL, high-density lipoproteins; ROS, reactive oxygen species; MDA, malondialdehyde; NO, nitric oxide; SOD, superoxide dismutase enzyme; GSH, reduced glutathione.

* Corresponding author at: Medical Parasitology Department, El Mowasah Medical and Educational Complex, Faculty of Medicine, Alexandria University, Alexandria, Egypt.
E-mail address: siak_1380@yahoo.com (S.I. Khedr).

Peer review under responsibility of King Saud University.

Production and hosting by Elsevier

https://doi.org/10.1016/j.sjbs.2020.10.026
1319-562X/

Invading pathogens, including *G. lamblia* lead to generation of free radicals including reactive oxygen species (ROS) in their host tissues as a defense mechanism, causing oxidative stress, with resultant lipid peroxidation (Mustafa et al., 2003; Forrester et al., 2018). Malondialdehyde (MDA) is the final product of lipid peroxidation, thus, it is measured as an oxidative stress marker (Todorova et al., 2005). Nitric oxide (NO) is another free radical that is generated during *Giardia* infection in many cells as it has antimicrobial capacity (Pavanelli et al., 2010). Antioxidants are effective free radicals' scavengers and ROS suppressors that are known to protect against reactive parasite-induced oxygen species. Superoxide dismutase enzyme (SOD) is an important enzymatic antioxidant, while reduced glutathione (GSH) is a non-enzymatic antioxidant which is synthesized in the liver (McCord and Fridovich, 2014; Pisoschi and Pop, 2015).

Many drugs are used to treat giardiasis. However, metronidazole remains the mainstay treatment. Yet, the reported side effects of the currently used drugs, together with the drug resistance necessitate searching for less harmful natural therapeutic anti-giardia alternatives (Tian et al., 2010; Neiva et al., 2014; Leitsch, 2015).

For ages, people relied on traditional medicine, especially plant extracts in treating health issues (Farnsworth, 1988). *Psidium guajava* Linn. (*P. guajava* L.) (guava) is a widespread evergreen tree that belongs to Myrtaceae family. Different tree parts possess a lot of medicinal properties that made it not only consumed as food but also used for long history as a traditional medicine to remedy various ailments (Naseer et al., 2018).

Preparations of guava leaves, in particular, have been used for treatment of various gastrointestinal disturbances, because, leaf extracts possess anti-microbial, anti-inflammatory, and antioxidant properties (Gutiérrez et al., 2008; Díaz-de-Cerio et al., 2017). Guava leaf anti-microbial properties were proven against various protozoa (Lee et al., 2013; Kaushik et al., 2015). There are different types of *P. guajava* leaf extracts, that vary according to the extraction method. The ethanolic extract contains the maximum phytoconstituents, thus it possesses a high medicinal potential (Arya et al., 2012).

The HPLC analysis of the ethanolic extract of Egyptian *Psidium guajava* L was performed recently by Taha et al., 2019. The authors demonstrated the phenolic compounds in the extract. They were; gallic acid, caffeic acid, coumaric acid, ferulic acid, cinnamic acid, resorcinol, chlorogenic acid and syringic acid. Their concentrations were as follow; 4.71, 4.37, 3.82, 3.55, 3.49 3.09, 2.93, and 2.85 μg/mg, respectively. Moreover, seven flavonoids were identified in the extract. Quercetin, hesperetin, kaempferol, quercitrin and rutin recorded the highest concentration, being; 8.94, 7.61, 7.55, 7.13 and 6.37 μg/mg, respectively. These were followed by catchin and apigenin with concentrations of 5.12 and 4.83 μg/mg of the extract. Three alkaloids were also identified, being; kaempfertin and isoquinoline in concentration of 1.89 and 1.24 μg/mg and corilagin that had the highest concentration (2.13 μg/mg). Thus, it can be concluded that flavonoids presented the highest fraction of PGLE, especially quercetin which is a powerful antioxidant agent (Taha et al., 2019).

The *in-vitro* efficacy of *Psidium guajava* leaves extract (PGLE) against *G. lamblia* was previously evaluated with promising results (Ponce-Macotela et al., 1994; Neiva et al., 2014). Yet, the *in-vivo* efficacy of PGLE has been rarely illustrated (De Souza, et al., 2014). Therefore, this study was designed to evaluate, the possible *in-vivo* therapeutic efficacy of PGLE against *Giardia lamblia* infection, with demonstration of the extract impact on serum liver enzymes, total bilirubin, albumin, lipid profile, liver oxidative stress biomarkers and intestinal inflammatory markers.

2. Material and methods

2.1. Collection, preservation and purification of Giardia cysts

Giardia lamblia cysts were obtained from stool samples collected from patients attending the outpatient clinics of National Medical Institute, Damanhour, Egypt. Samples were saline-emulsified and filtered. The suspension was centrifuged at 400*g* for 10 min, the resultant sediment was stored in 2.5% potassium dichromate solution at 4 °C (Eissa and Amer, 2012). Cysts were concentrated using sucrose flotation method (Amer et al., 2014), then were counted using a hemocytometer. The concentration process was repeated with more stool samples till obtaining a suspension containing 2×10^6 cysts/mL of Phosphate-buffered saline (PBS) (Dyab et al., 2016).

2.2. Preparation of Psidium guajava leaf ethanolic extract and the used concentration

Psidium guajava leaves were collected from their natural habitats in El-Ismailia, Egypt, during the summer season, 2018. A voucher specimen was deposited, authenticated and kept in the Herbarium of Faculty of Science, Alexandria University, Egypt. Leaves were dried in an air circulation oven at 38 °C, then, ground to obtain fine powder. Extraction was done by maceration and percolation using 70% ethanol (200 g/1L). The resultant extract solution was concentrated under reduced pressure in a rotary evaporator, then filtered, and stored in sterile bottles at 4 °C (Neiva et al., 2014). A pilot study was performed using; 25, 50 and 75 mg of the extract/kg. The best results were obtained using 75 mg/kg.

2.3. Assessment of total phenolic and flavonoid content in the extract

The total phenolic content in PGLE was determined using the method of (Taga et al., 1984). It was expressed as equivalents of gallic acid. The phenolic acid concentration obtained from PGLE was compared with standards. The flavonoid content was assessed using the method of (Moreno et al., 2000). Quercetin was used as a standard for estimating flavonoids. A triplicate of analyses was carried out and calculated

2.4. Control treatment for giardiasis

Metronidazole tablets (MNZ) (500 mg) (Flagyl®) (Sanofi Aventis Co.) were used as a therapeutic control. Tablets were finely ground and dissolved in PBS. Drug concentration was adjusted to 15 mg/kg/day for one-week post-infection (PI) (Dyab et al., 2016).

2.5. Experimental design

Fifty male Swiss-albino mice, aged 6 weeks and weighing 25 ± 3 grams underwent this study. Mice were first proven free from any parasitic infection, by the examination of three consecutive fecal samples on alternate days. Animals were housed in clean well-ventilated cages, with normal dark/light cycle. Room temperature was at 26 ± 2 °C. Rodent pellet diet and water were allowed *ad-libitum*, and beddings were daily changed.

Mice were divided into **five groups** (10 mice in each); **GI:** non-infected, **GII:** *Giardia*-infected and non-treated, **GIII:** *Giardia*-infected and treated with 15 mg of MNZ/ kg/ day, **GIV:** *Giardia*-infected and treated with 75 mg of PGLE /kg/day, and **GV:** *Giardia*-infected and treated with both drugs at the same doses.

Infected mice were individually, intraesophageally, inoculated with 2×10^5 *G.lamblia* cysts /0.1 mL. Starting from the 3rd day post

inoculation, stools of the inoculated mice were examined for *Giardia* cysts, to confirm that the infection has occurred. Treatments were started on the 6th day PI, and continued for one-week (Abdalla et al., 2011). Following the end of therapy, mice were kept fasting for 12 hours, anesthetized and sacrificed to assess the treatment efficacy.

2.6. Assessment of the treatment efficacy

The following parameters were assessed in the five groups;

2.6.1. Fecal Giardia cyst viability testing

This was performed just before sacrifice where, 0.1 gm of freshly voided stools from each infected mouse was thoroughly homogenized in 1 mL of saline. Then, the stools were stained using 0.3% Trypan Blue stain. The dark blue stained (dead cysts) and the unstained (alive cysts) were counted on Neubauer hemocytometer (Eissa and Amer, 2012).

2.6.2. Giardia trophozoite count

Trophozoites were counted in the mice' intestinal wash. The small intestines of the sacrificed mice were placed in sterile chill-iced saline. Tubes were vortexed to ensure trophozoites' release from the intestinal wall (Amer et al., 2014). Intestinal tissue was then gauze-filtered to separate trophozoites, which were counted using a hemocytometer. Four separate grids were counted for each mouse, with one parasite on one grid corresponded to 10^4 trophozoites/mL. Count was expressed as the number $\times$ 10^4 trophozoites/mL of intestinal wash (Abdalla et al., 2011).

2.6.3. Giardia trophozoite ultrastructural study

The retrieved trophozoites were fixed in cold $_4F_1G$ (formalin/glutaraldehyde), and processed for examination by scanning electron microscopy (SEM) and transmission electron microscopy (TEM) (Hayat, 2000).

2.6.4. Duodenal histopathological examination

Fresh duodenum tissues were excised, saline-washed and fixed in 10% neutral buffered-formalin for 24 hours. Specimens were dehydrated using ascending ethyl-alcohol concentrations. Paraffin-embedded, 4-µm-tissue sections were cut and stained with hematoxylin and eosin (H&E) (Shukla et al., 2010).

Sections were examined and photographed. To estimate the quantitative alterations, 5 boundaries from well labelled, non-overlapping areas were randomly chosen/slide/ 3 slide for each animal. A total of 15 boundaries/group were used. The parameters of inflammatory cell infiltration, vasodilatation, and the presence of hemorrhagic areas, edema, ulcerations and abscesses were determined and graded according to Kolli et al., 2013, as follows: **Score 1**—normal epithelium and connective tissue without vasodilatation; absence of or discreet cellular infiltration; and absence of hemorrhagic areas, ulcerations or abscesses; **Score 2**—discreet vasodilatation and areas of re-epithelization; discreet inflammatory infiltration with mononuclear prevalence; and absence of hemorrhagic areas, edema, ulcerations or abscesses; **Score 3**—moderate vasodilatation, areas of hydropic epithelial degeneration; inflammatory infiltration with neutrophil prevalence; edema and eventual ulcerations, and absence of abscesses; and **Score 4**—severe vasodilatation; inflammatory infiltration with neutrophil prevalence, edema, ulcerations, and abscesses.

2.6.5. Duodenal immunohistochemical study (IHC) for tumor necrosis factor-alpha (TNF-α)

Ten duodenum tissue sections/group were randomly selected, deparaffinized and hydrated. IHC was performed using Immune Cruz™ mouse LSAB Staining System (Code: sc-2050). Monoclonal mouse anti-TNF-α monoclonal antibodies, Santa Cruz Biotechnology, Inc, USA (Code: sc-52746) were used as primary antibodies in a dilution of 1:50. TNF-α expression intensity in positively stained cells was quantified using NIH Image J1047v software (10 fields/slide were measured, fields from well labeled, non-overlapping areas were randomly examined). Untreated sections with primary antibody of TNF-α were used as negative controls.

2.6.6. Scanning electron microscopic study of the duodenal villi and estimation of the mean villus length

Small pieces of fresh duodenum tissue were immediately fixed in cold $_4F_1G$ for 3 hours, then in 2% osmium tetroxide in the same buffer for 2 hours at 4 °C. Fixed samples were washed and dehydrated in a serial ethanol, mounted using carbon paste on an aluminum-stub and coated with gold-palladium in a sputter coating unit (JFC-1100 E). Specimens were then visualized using SEM-JSM-5300 (Hayat, 2000). To estimate mean villus length for each group, ten villi/section were measured and ten boundaries/slide/-mouse were examined.

2.6.7. Biochemical assessment

Blood samples were withdrawn from the sacrificed mice' hearts and left to clot, then, centrifuged to obtain clear sera, to measure liver enzymes (AST, ALT), total bilirubin and albumin concentrations using the methods of (Huang et al., 2006), (Rutkowski and Debaare, 1966), and (Grant, 1987), respectively. Moreover, serum total cholesterol, high-density lipoproteins (HDL), low-density lipoproteins (LDL) and triglycerides (TG) were measured using the methods of (Richmond, 1973), and (Bucolo and David, 1973). Liver enzymes' activity was expressed as (U/L), serum albumin was expressed as (g/dl), while total bilirubin values and lipid profile parameters were expressed as (mg/dl).

Additionally, liver tissue homogenates were prepared in 10 volumes of 0.1 M Tris-EDTA buffer, centrifuged at 4 °C. Supernatants were utilized for spectrophotometric assessment of liver concentration levels of; MDA, NO, and GSH using the methods of (Ohkawa et al., 1979), (Montgomery and Dymock, 1961) and (Beutler, 1963), respectively. Moreover, SOD activity was measured according to Nishikimi et al., 1972. Liver MDA was expressed as nmol /gm tissue, NO as (µmol / L), GSH as mg/gm tissue and SOD enzymatic activity was expressed as U/gm tissue.

2.7. Statistical analysis

Quantitative data were analyzed using F-test (ANOVA) and post-hoc test (Scheffe) for pairwise comparison. Data are expressed as means ± SD. $P < 0.05$ was considered statistically significant. All statistical calculations were performed using IBM SPSS software package version 20.0 (SPSS Inc, Chicago, IL, USA).

3. Results

3.1. Assessment of total phenolic and flavonoid content in the extract

Preliminary phytochemical analysis of PGLE showed the presence of total phenolic content of 386.5 mg gallic acid equivalent (GAE)/gram of the extract and flavonoids content of 265.9 mg quercetin equivalent (QE)/gram of the extract.

3.2. Giardia cyst viability

Viable *Giardia* cysts appeared very faint blue with apparent nuclei and an axostyle using Trypan Blue (Fig. 1.a). Dead cysts became swollen and dark blue with vague contents, indicating their death (Fig. 1.b). Recorded viability in the treated groups were

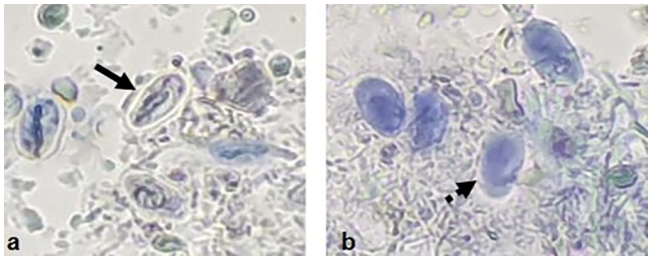

Fig.1. *Giardia lamblia* cysts in mice stools stained with Trypan Blue (×1000). (a) Viable *G. lamblia* cysts (arrow) were stained faint blue with apparent nuclei and an axostyle. (b) Dead *G. lamblia* cysts (arrow) were stained dark blue, with vague contents.

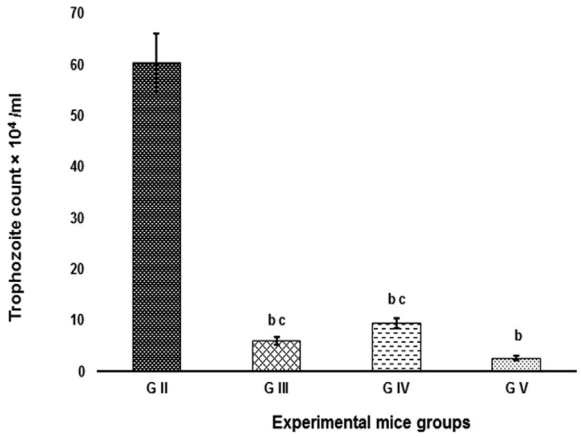

Fig.2. *Giardia lamblia* trophozoites count in small intestinal contents in different groups. n = 10 animals/group. Bars with different letters show statistically significant differences between the groups. b: means that there is a significant difference between the tagged group and group II, c: means that there is a significant difference between the tagged group and group V. ($P < 0.05$).

7.66%, 12.6% and 3.8% of the excreted fecal cysts in groups **III**, **IV** and **V** respectively.

3.3. Giardia trophozoite count

The mean trophozoite count in **GII** (the non-infected group), was 60.50 ± 5.57 × 10^4/ mL. The treated groups showed significant count reduction when compared with GII. **GV** (treated with both), showed the highest percentage reduction being; 95.72% with mean count of 2.59 ± 0.44 × 10^4/ mL. This was followed by **GIII (treated with MNZ)** with percentage reduction of 90.07% and mean count of 6.01 ± 0.82 × 10^4/ mL. The percentage reduction in **GIV (treated with PGLE),** was 84.36% with mean count of 9.46 ± 0.94 × 10^4/ mL. Interestingly, a significant difference was recorded between GV and GIII (Fig. 2) $P < 0.05$.

3.4. Giardia trophozoite ultrastructural study

Using SEM, *G. lamblia* trophozoites retrieved from **GII** showed their ubiquitous appearance; the suction-cup like adhesive disc that covers the ventral surface, smooth dorsal surface and flagella (Fig. 3 a,e,i). **GIII** trophozoites exhibited ventral disc fragmentation with appendage-like formation (long protrusions), cut flagella (Fig. 3b, j). Dorsal surface showed scattered papillae (shorter protrusions), erosions (superficial sloughing) and ulcers (deeper) (Fig. 3f). While, **GIV** trophozoites showed extensive blebbing on the surface, extending to the flagella (Fig. 3 c,g,k) with cut flagella (Fig. 3c) and dorsal surface erosions (Fig. 3g). Filopodium-like protrusions were detected (Fig. 3g). **GV** trophozoites were occasionally stunted and lost their pear shape with disfigured edematous disc and ill-defined ridge (Fig. 3d). Scattered papillae and appendages were seen (Fig. 3d, h,l) with deep ulceration (Fig. 3h,l). Lost or swollen flagella (Fig. 3 d,h) were seen.

Under TEM, **non-treated** *G. lamblia* trophozoites displayed its typical structure, with two nuclei, ventral disc, peripheral vesicles

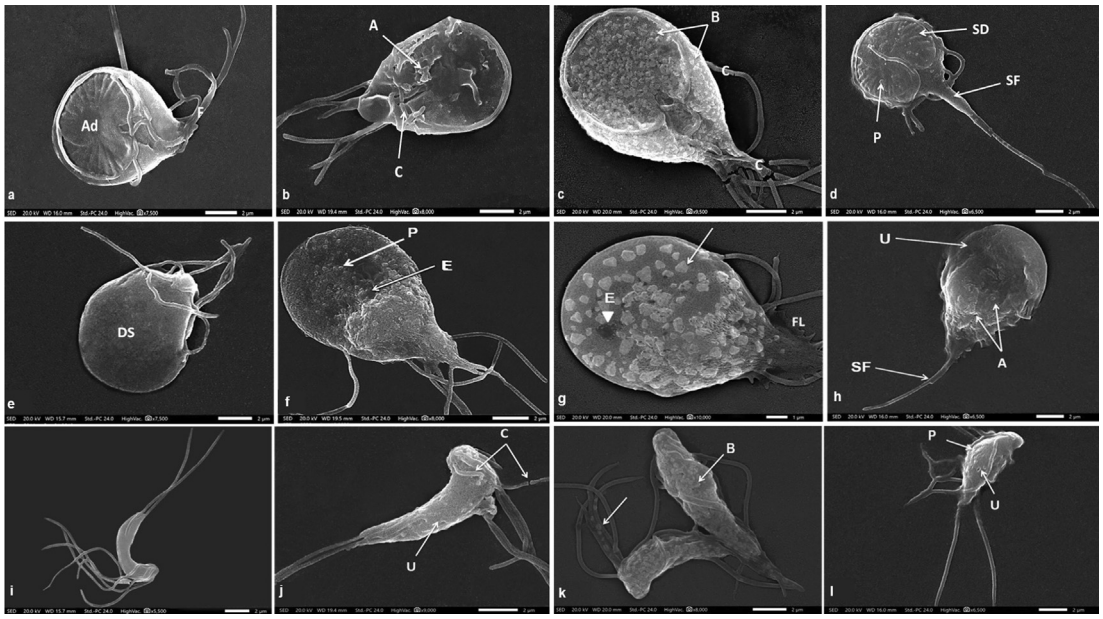

Fig. 3. SEM features of *G. lamblia* trophozoites in different groups. **a-d: SEM of the trophozoite ventral surface a:** GII trophozoite showing concave adhesive disc **(Ad)**, with ventral and caudal flagella **(F)** (7500×). **b:** MNZ-treated trophozoite showing rough ventral disc with papillae and appendages **(A)** and cut flagella **(C)** (8000×). **c:** PGLE-treated trophozoite showed extensive ventral surface blebbing **(B)** with cut flagella **(C)** (9500×). **d: GV** trophozoite was stunted with disfigured edematous sucking disc **(SD)** and ill-defined ridge, swollen caudal flagella **(SF)** and papillae **(P)** (6500×). **e-h: SEM of the dorsal surface e:** non-treated trophozoite showing smooth dorsal surface **(DS)** (7500×). **f:** GIII trophozoite, showing swelling, dorsal surface irregularity, and erosions **(E)** and papillae **(P)** (8000×). **g: GIV** trophozoite showing extensive blebbing **(B)**, erosions **(E)** with filopodium like protrusions **(FL)** (10,000×). **h:** GV trophozoite showing irregular ulcerated **(U)** surface, with papillae **(P)**, appendages **(A)**, with swollen caudal flagellum **(SF)** (6500×). **i-l: SEM features of trophozoite lateral view i:** non-treated trophozoite showing smooth surface with eight flagella (5500×). **j:** MNZ-treated trophozoite is swollen with irregular ulcerated surface **(U)** and cut flagella **(C)** (9000×). **k:** PGLE-treated trophozoite with extensive blebbing **(B)**, extending to the flagella (arrows) (8000×). **l:** GV trophozoite showing papillae **(P)**, and ulcers **(U)** (6500×).

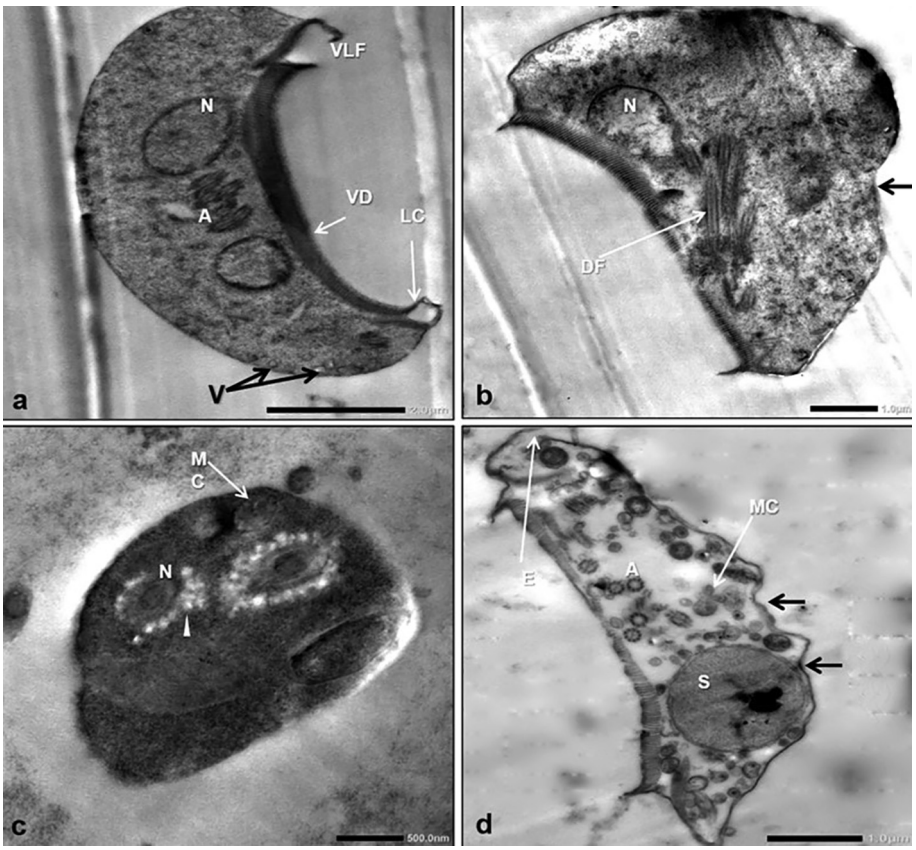

Fig. 4. TEM micrographs of *Giardia* trophozoites in different groups. **a: GII** trophozoite, with striated ventral disc **(VD)**, lateral crest **(LC)** and ventrolateral flange **(VLF)**, 2 nuclei **(N)**, peripheral vesicles **(V)** immediately below the plasma membrane, and flagellar axonemes **(A)**. **b:** Swollen GIII trophozoites showing irregular ulcerated surface **(arrow)**, lost nuclear integrity **(N)** and disorganized flagella **(DF)**. **c:** PGLE-treated trophozoites showing dispersed fat droplets **(arrow head)** within the body especially *peri*-nuclear, with membrane bound cavities **(MC)**. **d:** GV trophozoite, showing irregular surface **(black arrow)**, membrane erosion **(E)**, disorganized flagellar arrangement, dissolution of one nucleus and swelling of the other nucleus **(S)** (5000×).

beneath the plasma membrane, flagellar axonemes that show proximity to the nuclei (Fig. 4a). **MNZ-treated** trophozoites were swollen with irregular surface membrane, lost nuclear integrity and disorganized flagella (Fig. 4b). **PGLE-treated** trophozoites lost its normal architecture and showed dispersed fat droplets especially around the nuclei and axonemes. Membrane bound cavities were also noted (Fig. 4c). Severe trophozoite damage was noted in **GV**, with loss of plasma membrane integrity. Loss of the normal architecture and dissociation of the intracytoplasmic components were evident. Swelling or dissolution of nuclei were obvious, with disorganized flagellar arrangement (Fig. 4d).

3.5. Duodenal histopathological examination

The normal duodenal histological observations of H&E-stained sections of **GI** are represented in Fig. 5a, with normal crypts and muscular architecture. The duodenum villi had shown normal histological architecture with intact tall columnar epithelium and regularly arranged nuclei and normal finger-like villi, without villus atrophy nor inflammatory response in the lamina propria were noted. In contrast, **GII** showed short and blunt intestinal villi with loss of normal villus and crypt architecture. The height of the epithelial columnar cells was reduced and their nuclei have lost the normal polarity, with irregular pyknotic nucleoli. Duodenal mucositis and ulceration were seen. Lamina propria showed many inflammatory cells, chiefly lympho-mononuclear. *Giardia* trophozoites were seen as slender crescents in close vicinity to the damaged area, in between the villi, along the mucosal surface, arranged in clusters, entrapped in mucus, or free in the lumen (Fig. 5b-d).

Duodenal sections of **GIII** achieved great improvement in the pathological mucosal changes, with less inflammatory infiltrate (Fig. 5e). Regarding **GIV** duodenal histological sections, almost near normal villus and crypt architecture were obvious with preserved mucosal layer and less lymphocytic infiltration (Fig. 5f). Interestingly, **GV** duodenal sections showed remarkable preservation of duodenal tissue, with restoration of normal villi and crypts architecture. Lymphocytic infiltration was very mild and no trophozoites were seen (Fig. 5g). The histopathological scores confirmed a significantly higher inflammation rate and tissue damage in the duodenum of **GII** mice (infected, non-treated) relative to those of control group (**GI**). The three treated groups showed significantly decreased microscopic injury score when compared to **G II** ($P < 0.05$) (Fig. 5h).

3.6. Duodenal immunohistochemical study (IHC) for Tumor necrosis factor-alpha (TNF-α)

In **GI**, few duodenal cells showed faint positive TNF-α expression manifested as brown coloration (Fig. 6a). A significant increase in TNF-α expression in **GII** was shown (Fig. 6b), when compared to GI. On the other hand, **GIV** and **GV** (Fig. 6 d, e) showed a significant reduction in TNF-α expression, compared to GII, particularly in the villi apical parts. The highest TNF-α expression was met in GII and the least expression was in GV (Fig. 6f). ($P < 0.05$)

3.7. Duodenal villus SEM and estimation of the mean villus length

Fig. 7a shows the healthy duodenal villi of **GI**, arranged in close array and lying almost parallel to each other. Vigorous duodenal

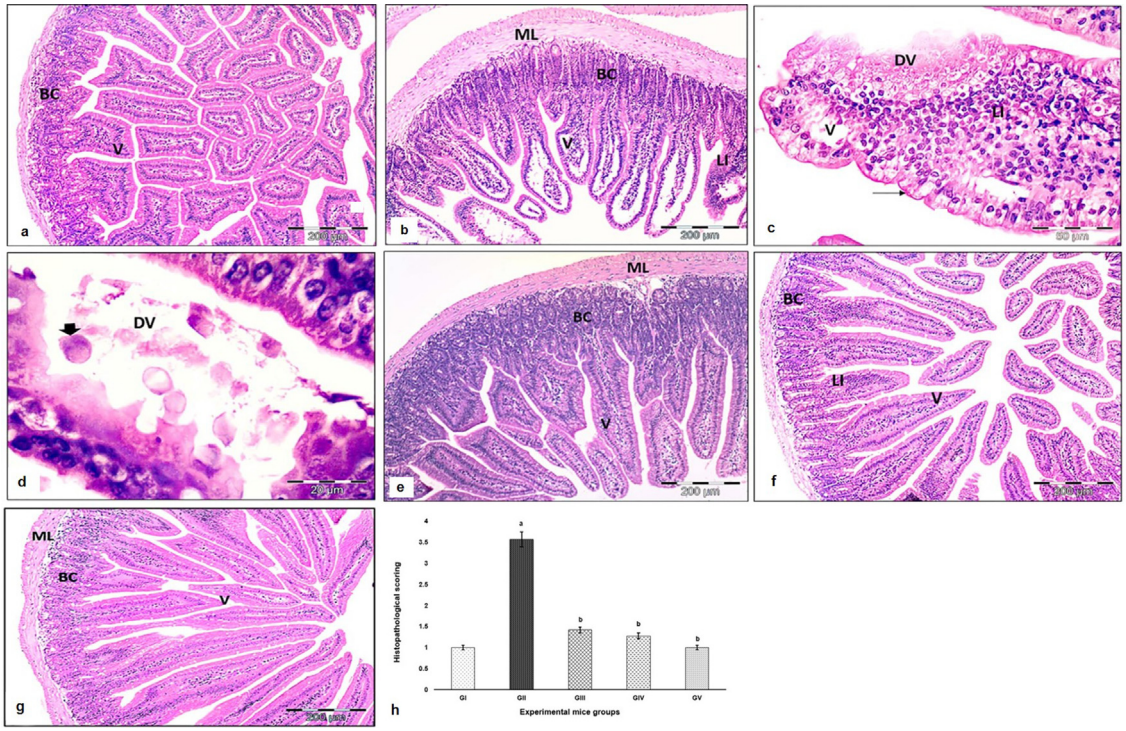

Fig.5. H&E-stained duodenal histological findings. **a: GI** showing intact mucosal layer, finger patterned villi **(V)**, and basal crypts **(BC)**. **b: GII** duodenum showing absence of the normal villus **(V)** architecture, with damaged muscular layer **(ML)**, elongated crypts **(BC)**. **c: GII** showing dissolved villi tips with damaged villi **(DV)**, heavy lymphocytic infiltration **(LI)** in the lamina propria. Vacuolation **(V)** of epithelial cells and erosion of villus brush border **(thin arrow)**. **d:** Shedding of the duodenal epithelium with severe villus damage **(DV)** and ulceration. Trophozoites are seen **(arrow heads)**. **e: GIII**, showing intact muscular layer **(ML)**, preserved villus architecture **(V)** and basal crypts **(BC)**, with minimal cellular. **f: GIV** showing well-preserved basal crypts **(BC)**, normal villus architecture **(V),** intact mucosal epithelium and some lymphatic infiltration **(LI)**. **g: GV** exhibited normal morphology of the basal crypts **(BC)**, intact mucosal epithelial lining **(V)**. **h:** Scoring of histology sections. Results are expressed as mean ± SE. Bars with different letters show statistically significant differences between the groups ($P < 0.05$). **h:** Morphometric measurements of villus length. n = 6 animals/group were examined. Bars with different letters show statistically significant differences between these groups.

mucosal abnormalities were observed in **GII** (Fig. 7 b-e), with villus atrophy and stunting. Villus ridges were not distinctly recognizable. Severely damaged, disoriented microvilli with deposition of cellular exudates were utterly obvious. Pear-shaped trophozoites measuring around 15 X 7 μm were seen clasped in-situ by their sucking discs, bulging above the brush border and aggregated in close vicinity to villi bases. Impressions produced by trophozoites' suction discs were visible. *G. lamblia* cysts were not detected. Villi of **GIII** and **GIV** showed improved morphology (Fig. 7 f, g). Importantly, **GV** villi showed pronounced architecture improvement with better microvilli arrangement (Fig. 7 h). No trophozoites were detected in the treated groups.

Morphometric measurements showed significant differences in **villus length** among groups ($P < 0.05$) (Fig. 7i). A significant decrease in **GII** villus length relative to **GI** was observed. The highest villus length in the treated groups was achieved in **GV**, being, 360.31 μm ± 8.32, this was followed by **GIV**, being, 349.78 μm ± 11. 86. Interestingly, the villus length achieved by MNZ-treatment in **GIII** was 338.65 μm ± 5.02, which was significantly lower than PGLE-treated groups.

3.8. Biochemical assessment

Mean serum enzymatic activities of AST and ALT showed a significant increase in **GII** when compared to **GI**. Furthermore, a significant decrease in **GIV** and **GV** enzyme levels was detected when compared to GII. Contrarily, a significant increase in AST and ALT was noted in **GIII** when compared to GII (Fig. 8a). No significant changes were detected in total bilirubin nor in albumin levels among the treated groups neither when compared to GI, nor, when compared to GII (Fig. 8 b, c).

Concerning lipid profile parameters, a significant reduction was obtained in total cholesterol, HDL, LDL and TG in **GII**, with a slight increase in **GIII**, **GIV** and **GV**, yet lipids remained within the normal range (Fig. 9). Interestingly, total cholesterol, LDL and TG levels were less in **GIV** that received PGLE than in **GIII** that received MNZ.

Hepatic oxidative stress results are shown in (Fig. 10 a-d). Both MDA and NO showed significant increase in **GII** and a significant decrease in **GV**. The reverse was shown in case of antioxidant profile, where, GSH and SOD showed significant decrease in **GII** and a significant increase in **GV.** The used *P* value for biochemical assessment is < 0.05.

4. Discussion

Giardia lamblia has been, for years, the most prevalent protozoan causing gastroenteritis, especially in the developing countries (Oppong et al., 2020). Bearing in mind the side effects of the reference anti-giardia drugs and the resistance against them, the necessity to search novel, safe, and effective agents to treat giardiasis becomes imperative. Thus, traditionally-used plants for treatment of gastrointestinal disorders would be ideal alternative therapies (Amaral et al., 2006).

Searching for this alternative, the current authors found that PGLE antiprotozoal effect has been, fortunately, previously emphasized in multiple works. Adeyemi et al., 2011 suggested that PGLE has a trypanocidal activity against *Trypanosoma brucei brucei* that is comparable to the reference drugs. Kaushik et al., 2015 proposed the leaves as an anti-malaria agent. Besides, the effect of guava leaf essential oil against toxoplasmosis was reported (Lee et al., 2013).

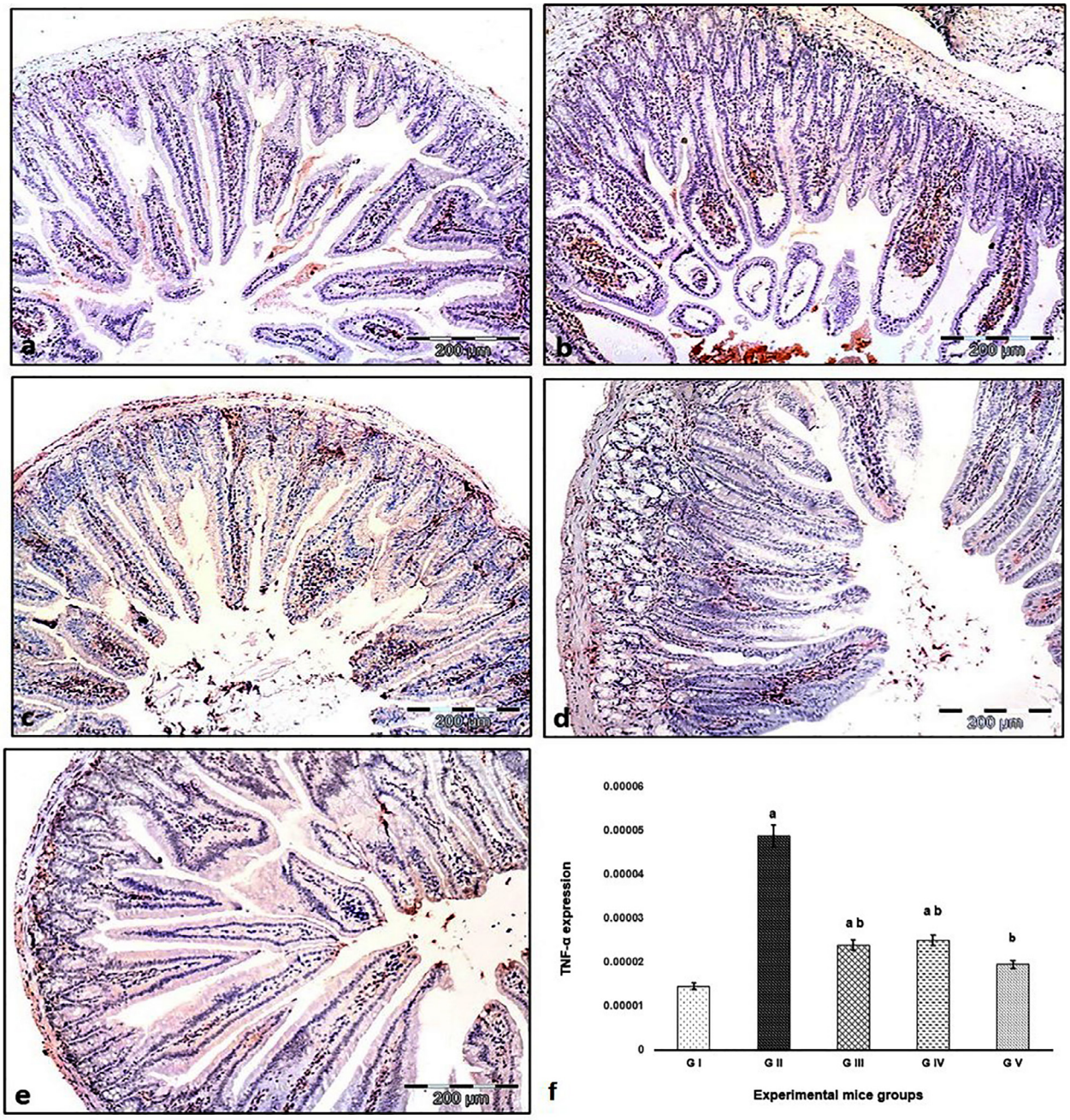

Fig.6. Duodenal epithelial immunohistochemical analysis for TNF-α **a: GI** showing faint TNF-α expression. **b: GII** showing TNF-α over-expression, seen as brown color. **c&d:** showing little TNF-α expression in **GIII & GIV**. **e: GV** showing the least TNF-α expression among the treated groups. **f:** TNF-α expression levels of n = 6 animals/group. Bars with different letters show significant differences between the groups ($P < 0.05$).

Furthermore, Neiva et al., 2014 has proved the in-vitro anti-giardia effect of PGLE.

Accordingly, the *in-vivo* anti-giardia effect of PGLE, that is deficient in literature, was studied herein, thus, extending the range of protozoan species that could be targeted by PGLE. Indeed, there are different types of *P. guajava* leaf extracts, that vary according to the extraction method. The ethanolic extract was chosen in the current work because according to Arya et al., 2012, it contains the maximum phytoconstituents with their medicinal properties.

Considering that acute giardiasis usually peaks in about one-week PI (Halliez and Buret, 2013), the current treatment was started in the 6th day PI, and was then continued for seven successive days. On calculating the trophozoite count in the treated groups, following the end of therapy, the intestinal parasite density was, noticeably, significantly reduced in **GIV** that received PGLE. Birdi et al., 2011 proved the *in-vitro* potential anti-giardia effect of PGL decoction. In the same context, Neiva et al., 2014 concluded that the hydroethanolic PGLE showed moderate *in-vitro* anti-giardia activity at a concentration of 500 µg/mL. Interestingly, on testing the *in-vitro* anti-giardia PGLE activity, Ponce-Macotela et al., 1994 found that the caused *Giardia* mortality rate was significantly superior than that caused by tinidazole.

Yet, the current reduction in the intestinal parasite burden in **PGLE-treated** group was less than the percentage reduction in **MNZ-treated** group. Interestingly, the best reduction was obtained by the combined therapy. This effect was explained by

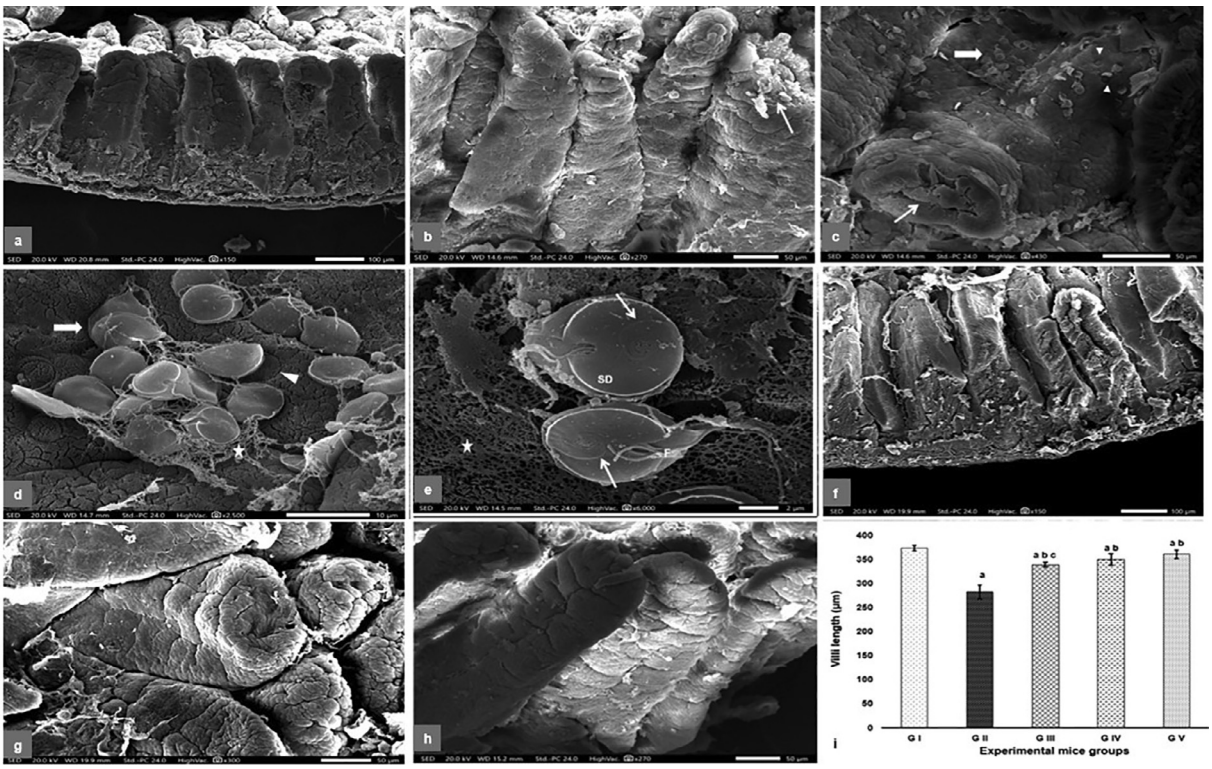

Fig.7. Duodenal mucosal SEM. **a: GI** exhibited well-organized finger-like villi (150×). **b-e: GII** where, **b:** shows damaged and blunt microvilli, peeling of the epithelial cells and reduction of the villus length, the white arrow points to eroded, widened villus tips (270×). **c:** *G. lamblia* trophozoites are seen in the close vicinity to the damaged villi, especially at the villus base **(thick arrow).** Impressions produced by suction discs are also visible **(arrow heads)** with villus tip peeling **(arrow)** (430×). **d:** Higher magnification of heavily infected duodenal villi with trophozoites, attached by their discs, leaving impressions **(arrow heads)** (2500×). **e:** Trophozoite ventral surface is shown, suction disc **(SD),** flagella **(F)** and spiral ridge (arrows), with the cellular exudates **(★)** deposited on damaged villi surface (6000×). **f: GIII** showing partially damaged villi of unequal length (150×). **g: GIV** showing improved villus morphology and orientation (300×). **h: GV** showing well-organized, properly distributed microvilli (270×). **i:** Morphometric measurements of villus length. n = 6 animals/group were examined. Bars with different letters show statistically significant differences between these groups ($P < 0.05$).

Miklasińska-Majdanik et al., 2018, who concluded that, natural polyphenols, aside from its direct antimicrobial activity, exert a synergistic effect on combination with chemotherapeutics. This explains why, herein, PGLE that is rich in natural polyphenols, has potentiated the effect of MNZ, the golden anti-giardia therapy (Diaz et al., 2012; Díaz-de-Cerio et al., 2017). Calzada et al., 2005 concluded that flavonoids in plants possess high giardicidal activity, accordingly, the presence of flavonoids in *P. guajava* leaves explains the current results. Flavonoids are amongst polyphenols' classes (Miklasińska-Majdanik et al., 2018).

The fact of being previously ethnopharmacologically heavily studied and proved safe, coupled with its good *in-vitro* giardicidal activity, both, make PGLE, in particular, one of the perfect medicinal plant options in giardiasis treatment. This fact was validated, herein, by not recording any animal deaths after a week of administration of 75 mg/kg PGLE/day, and also by the significant reduction in serum liver enzymes in the PGLE-treated groups. Both findings support the safety of the used extract at the given doses.

On ultrastructural verification of PGLE-treated trophozoites, surface blebbing and erosions were shown, this was potentiated when combined with MNZ, leading to sucking disc damage. Knowing that trophozoite attachment to the host small intestinal villi is mainly achieved by the sucking disc, corrupted disc is a finding that explains the massive count reduction in the treated groups. Trophozoite cell membrane injury leads to cytoplasm leakage, parasite swelling, and parasite death (Ponce-Macotela et al., 2006). PGLE damaging effect against *Giardia*was ascertained by TEM, where, **GIV** and **GV** trophozoites showed ultrastructural disorganization and cytoplasmic components' dissociation, nuclear dissolution, flagellar disorganization, and membrane erosion.

The histopathological duodenal lesions in **GII**, herein, coincide with data shown by (Buret, 2008). Besides, intraepithelial lymphocytic inflammatory infiltrate was noted, this is because the intestinal lymphocytes play an important role in the parasite clearance from the gut (Owen et al., 1979).

Improvement of the villus histopathological architecture was observed in all treated groups. Nevertheless, the best improvement resulted from combination therapy. Groups that received PGLE showed significantly higher villus length when compared to **GIII**. This improvement could be attributed to ulcero-protective activity of PGLE, that was proved by Tende et al., 2013. Naseer et al., 2018 showed that oral ulcers can be treated with PGLE. Jayakumari et al. (2012) attributed this anti-ulcer activity to the flavonoids in the extract.

The current highest TNF-α expression was met in **GII**, this is because the intestinal inflammation in giardiasis is mediated by pro-inflammatory cytokines including TNF-α (Goyal and Shukla, 2013), that plays a protective role in early giardiasis (Zhou et al., 2007). TNF-α production impairs epithelial integrity and thus contributes to digestive tract ulcer formation (Tourani et al., 2018). TNF-α also controls free radicals aiming at decreasing inflammation (Diaz et al., 2012). Thus, herein, intestinal epithelium ulceration in *Giardia*-infected mice was accompanied with high production of TNF-α in the lamina propria. Abdul-Wahid and Faubert, 2008 demonstrated that $CD4^{+}$T cells and their cytokines participate in *G. lamblia* infection control. Serradell et al., 2018 sta-

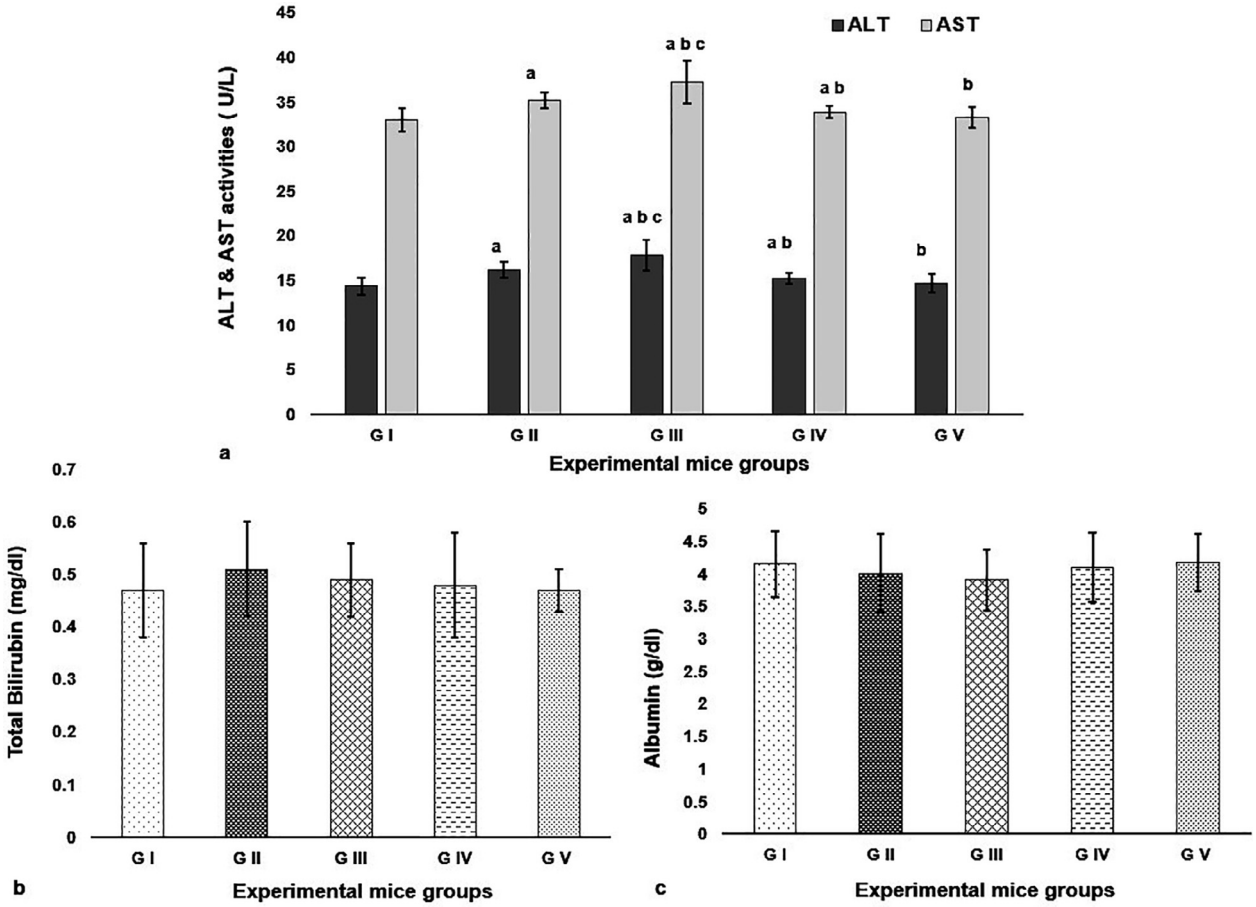

Fig.8. a: AST & ALT levels. **b:** Serum total bilirubin. **c:** Serum albumin level. n = 6 animals/group. Bars with different letters show statistically significant differences between these groups. a; means that there is a significant difference between the tagged group and group I, b: means that there is a significant difference between the tagged group and group II, c: means that there is a significant difference between the tagged group and group V. Data are expressed as means ± SD ($P < 0.05$).

ted that, during *Giardia* infection, intestinal cytokine responses showed a biphasic profile: an early induction of cytokines including TNF, with intestinal alterations typical for inflammation, followed by a shift toward a predominant Th2 response, associated with a counter-regulatory mechanism.

On the other hand, the currently reported low TNF-α in the treated specimens maybe a reflection for the few $CD4^+$ cells in the non-inflamed mucosa (Goyal and Shukla, 2013). According to de Araújo et al., 2014, the anti-inflammatory activity of PGLE reduces the leukocytic migration. This is why low TNF-α expression was met in PGLE-treated mice. Samardžić et al., 2018 stated that, the phytochemicals present in plants, mainly polyphenols, have anti-ulcer, antioxidant, and anti-inflammatory pharmacological properties.

The SEM of **GII** intestine revealed preferential aggregation of trophozoites at the sheltered places especially; villi tops and bases that offered mechanical protection from the flow of intestinal contents (Khanna et al., 1990). Interestingly, the ultrastructural mucosal changes observed in PGLE-treated mice showed healing of the mucosal changes previously caused by the infection.

Because most of the drugs are metabolized in the liver, serum levels of ALT, AST, total bilirubin and albumin were measured in the sera of current mice groups as clinical biomarkers for liver health secondary to PGLE administration. Our results revealed that there is a statistically significant increase in AST and ALT activities in **GII** and **GIII** when compared with **GI**. The highest hepatic enzymatic activity was met in **GIII** that received MNZ, this was significantly higher than **GII** enzymes. This finding was in agreement with Chon and Kim, 2005 and Oda, 2012. This increase in ALT, AST activities can be attributed to hepatocytes' cell membrane damage, leading to an increase in cell membrane permeability and facilitating the passage of cytoplasmic enzymes outside the cells, leading to their increase in the serum (Gaur and Bhatia, 2009). According to Elmadawy et al., 2016, *Giardia* induced a significant ALT and AST elevation. Interestingly, PGLE-treated mice showed significantly lower liver enzymes' levels. Chen et al., 2011 attributed PGLE hepato-protective activity to the preservation of the hepatocellular membrane structural integrity, thus, liver enzymes leakage into the circulation is prevented. Herein, the hepatoprotective activity of PGLE was validated via monitoring serum levels of AST, ALT and total bilirubin, revealing significantly better profiles in PGLE-treated group with ameliorated MNZ-induced hepatotoxicity in **GV**, this was in accordance with Mohamed, 2012, who found that PGLE had reduced drug-induced elevated hepatic enzymes. Noteworthy that, Kaneko et al., 2013, confirmed that, there is no possibility of interactions between PGLE and medicines due to its weak inhibitory effect on cytochrome P450, thus, weak effect on drug metabolism in liver. Accordingly, when combined with MNZ, PGLE will not diminish its efficacy.

The present total serum bilirubin and albumin levels did not show any significant changes in infected groups when compared with those of **GI**. Similarly, no significant changes were recorded between treated groups and **GII**. This may be due to the short duration of infection that was not enough to disturb total bilirubin and albumin levels (Aly et al., 2014; Muda and Atik, 2018).

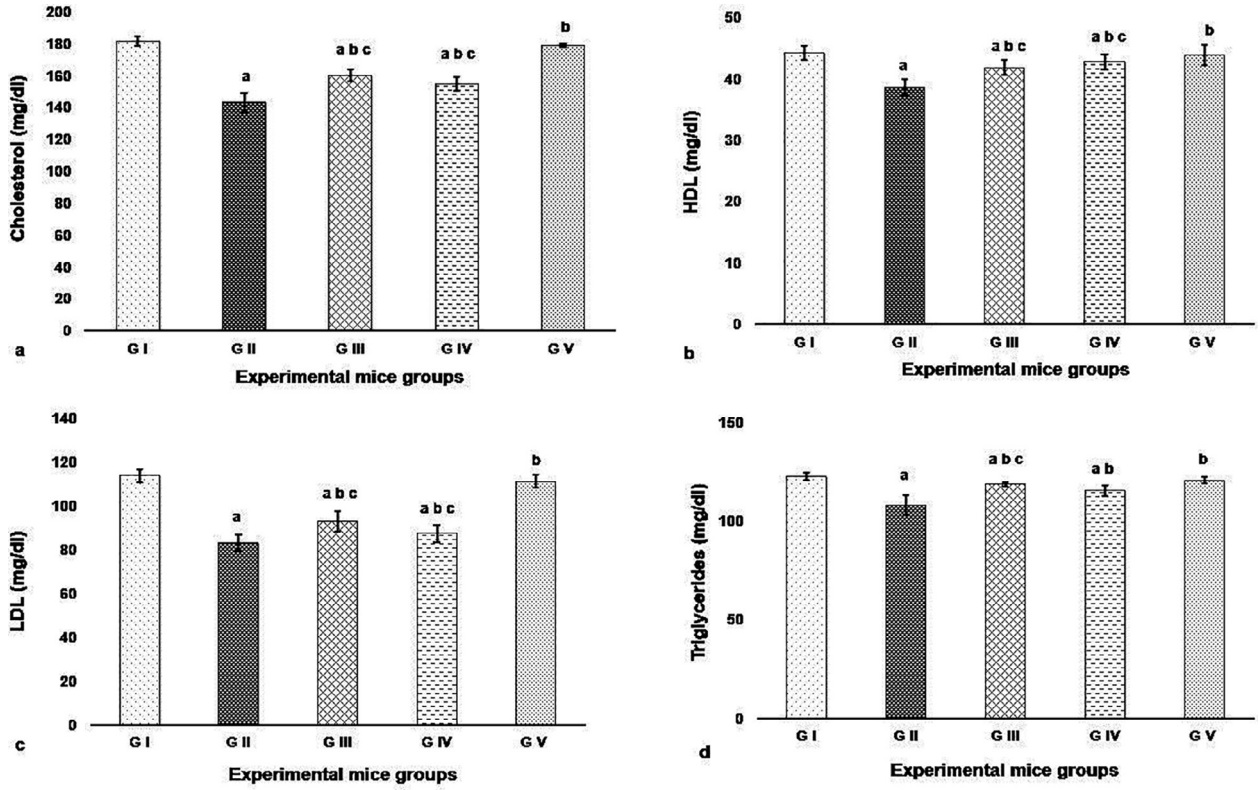

Fig.9. Serum lipid levels. **a:** Total cholesterol, **b:** HDL, **c:** LDL. **d:** TG. n = 6 animals/group.

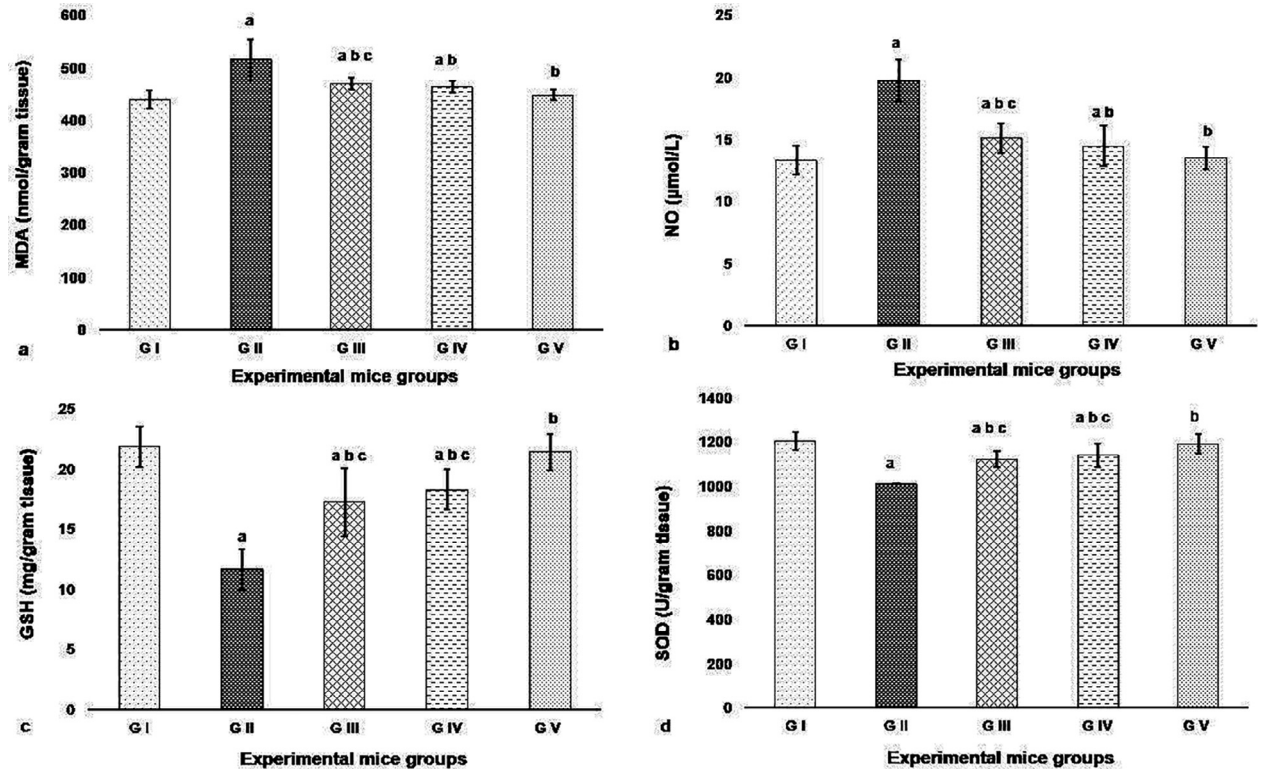

Fig. 10. Oxidative stress markers in different groups. **a:** MDA, **b:** NO, **c:** GSH and **d:** SOD. n = 6 animals/group.

Concerning current lipid profile, **GII** exhibited the least values of cholesterol and TG among the studied groups. This is because *Giardia* is unable to de-novo synthesize the majority of its own lipids and cholesterol, thus it consumes host lipids for energy production and membrane/organelle biosynthesis. Cholesterol is needed for trophozoite encystation in the intestine; thus, it is usually used up (Yichoy et al., 2011). The current results are similar to Bansal et al., 2005 who observed that *G. lamblia* infection lowers total

cholesterol, HDL and LDL levels than in healthy controls. Free fatty acids generated from TG are also detrimental to *Giardia* growth (Das et al., 1988).

The current treated groups; **GIII**, **GIV**, and **GV** showed increased cholesterol and TG when compared to **GII**, this can be attributed to the anti-giardia potential of MNZ and PGLE. Yet, levels were still within the normal range. Noteworthy that PGLE were proved to have hypolipidemic effect in case of hypercholesterolemia where they reduced the serum TG, total cholesterol and LDL levels and increased the HDL level (Akinloye et al., 2010; Tella et al., 2019). In giardiasis treatment, this is not the case, because the infection already causes hypocholesterolemia, thus, this hypolipidemic effect was masked. Nevertheless, herein, PGLE-treated group showed less total cholesterol, LDL and TG levels than in **GIII** that received MNZ.

PGLE was also proved to protect against oxidative stress induced by hypercholesterolemia (Freire et al., 2014), thanks to its abundant phenolic constituents, that are known to be active antioxidants (You et al., 2011). Thus, **GIV** and **GV** showed a significant increase in SOD activity and GSH content, with simultaneous decline in MDA and NO concentration levels. Suganya et al., 2007, found that PGLE exhibited strong free radical scavenging effects, which is a key factor in combatting oxidative stress. **GIII** showed significant amelioration in the hepatic oxidative stress markers; MDA and NO with significant increase in GSH content and SOD enzymatic activity, this was in accordance with Fahmy et al.,2019. This can be attributed to the antioxidant equilibrium that was attained as a result of the reduction in the free radical production by the host immune system, upon *Giardia* elimination,

On the other side, depletion of SOD and GSH, the mutually supportive antioxidants that protect against ROS was recorded in **GII**, perhaps as a consequence of the exhaustion of the host SOD and GSH in neutralizing the free radicals generated by the parasitic infection (Surai, 2016). This was in accordance with Kiran et al., 2019. According to previous studies, parasitic infections deplete the hepatic SOD (Bahrami et al., 2015). The high MDA in *Giardia*-infected mice could be explained as free radical damage evoking significant changes in the host oxidative status (Bahrami et al., 2015). Similarly, NO level shows its maximum in **GII**, maybe because it is responsible for host defense against *G. lamblia* infection, being inhibitory to trophozoite encystation and cyst excystation (Zarebavani et al., 2017).

5. Conclusion

This study highlights, the promising *in-vivo* giardicidal activity of PGLE, that was comparable to MNZ. Taking the current results into consideration, the studied extract would be an ideal treatment for giardiasis either as an alternative or in combination with MNZ. PGLE greatly helped in the healing of *Giardia*-induced gut atrophy, thus, offering a comprehensive therapy for giardiasis treating both the pathogen and the resultant pathological sequalae. When combined with MNZ the extract potentiated its therapeutic effect. Moreover, having anti-inflammatory, hepatoprotective and antioxidant properties, the extract can combat the side effects of MNZ therapy. Nevertheless, more studies are necessary to move forward in this way. Besides, an approach to formulate a combination therapy of MNZ and PGLE is essential to be easily administered in clinical practice.

6. Ethical approval and Informed consent

Stool specimens were collected as a part of patient clinical examination, according to the national guidelines. Informed consents were sought from patients. Approval from the institutional ethics committee was obtained. Animal experiments were done with strict accordance to the institutional ethical guidelines for care and use of animals in research.

Funding

This research did not receive any specific grant from funding agencies in the public, commercial, or not-for-profit sectors.

Declaration of Competing Interest

The authors declare that they have no conflict of interest.

Acknowledgement

Authors are thankful to Professor Dr. Eglal Amer, Professor of Medical Parasitology, Faculty of Medicine, Alexandria University, Egypt, for her great help and assistance in the current study. Great thanks extend to Professor. Salama El-Darier, Professor of Plant Ecology, Botany and Microbiology Department, Faculty of Science, Alexandria University, Egypt, for preparation of the extract used in this study.

References

Abdalla, S., Ramadan, N., Mohamed, A., El-Deeb, H., Al-Khadrawy, F., Badawy, A., 2011. A study on the effect of Myrtus communis and Olibanum on *Giardia lamblia* infection in Egypt. Parasitol. United J. 4 (1), 89–100.

Abdul-Wahid, A., Faubert, G., 2008. Characterization of the local immune response to cyst antigens during the acute and elimination phases of primary murine giardiasis. Int. J. Parasitol. 38 (6), 691–703. https://doi.org/10.1016/j.ijpara.2007.10.004.

Adeyemi, O.S., Sykes, M.L., Akanji, M.A., Avery, V.M., 2011. Anti-trypanosomal and cytotoxic activity of ethanolic extracts of *Psidium guajava* leaves in Alamar Blue based assays. Vet. Arch. 81 (5), 623–633.

Akinloye, O., Akinmoladun, A.C., Farombi, E.O., 2010. Modulatory effect of *Psidium guajava* linn and ocimum gratissimum Linn on lipid profile and selected biochemical indices in rabbits fed high cholesterol diet. J. Complement. Integr. Med., 7

Aly, E.M., Sabry, H.Y., Fahmy, Z.H., Zalat, R.S., 2014. Efficacy of combination therapy (metronidazole and/or artemether) in experimental giardiasis and its impact on nonenzymatic oxidative stress biomarkers. Parasitol. United J. 7 (1), 68.

Amaral, F.M., Ribeiro, M.N.S., Barbosa-Filho, J.M., Reis, A.S., Nascimento, F.R., Macedo, R.O., 2006. Plants and chemical constituents with giardicidal activity. Rev. Bras. Farmacogn. 16, 696–720. https://doi.org/10.1590/S0102-695X2006000500017.

Amer, E.I., Mossallam, S.F., Mahrous, H., 2014. Therapeutic enhancement of newly derived bacteriocins against *Giardia lamblia*. Exp. Parasitol. 146, 52–63. https://doi.org/10.1016/j.exppara.2014.09.005.

Arya, V., Thakur, N., Kashyap, C., 2012. Preliminary phytochemical analysis of the extracts of Psidium leaves. J. Pharmacogn. Phytochem. 1 (1), 1–5. https://doi.org/10.5829/idosi.mejsr. 2014, 19(11), pp. 11415.

Bahrami, S., Razi Jalali, M.H., Jafari, A., 2015. Evaluation of hepatic antioxidant changes in ovine dicrocoeliosis. J. Parasit. Dis. 39, 766–769. https://doi.org/10.1007/s12639-013-0415-1.

Bansal, D., Bhatti, H.S., Sehgal, R., 2005. Altered lipid parameters in patients infected with Entamoeba histolytica, Entamoeba dispar and *Giardia lamblia*. Br. J. Biomed. Sci. 62 (2), 63–65. https://doi.org/10.1080/09674845.2005.11732686.

Birdi, T.J., Daswani, P.G., Brijesh, S., Tetali, P., 2011. In vitro antigiardial and antirotaviral activity of *Psidium guajava* L. leaves. Indian J. Pharmacol. 43 (5), 616. https://doi.org/10.4103/0253-7613.84990.

Beutler, E., 1963. Improved method for the determination of blood glutathione. J. Lab. Clin. Med. 61, 882–888.

Bucolo, G., David, H., 1973. Quantitative determination of serum triglycerides by the use of enzymes. Clin. Chem. 19 (5), 476–482. PMID: 4703655.

Buret, A., 2008. Pathophysiology of enteric infections with Giardia duodenalius. 15 (3), 261-265. https://doi.org/10.1051/parasite/2008153261.

Cabal-Hierro, L., Lazo, P.S., 2012. Signal transduction by tumor necrosis factor receptors. Cell Signal. 24 (6), 1297–1305. https://doi.org/10.1016/j.cellsig.2012.02.006.

Calzada, F., Cervantes-Martínez, J.A., Yépez-Mulia, L., 2005. In vitro antiprotozoal activity from the roots of Geranium mexicanum and its constituents on Entamoeba histolytica and *Giardia lamblia*. J. Ethnopharmacol. 98 (1–2), 191–193. https://doi.org/10.1016/j.jep.2005. 01.019.

Chen, H.H., Wu, P.H., Lo, D., Pan, Y., Wu, M., 2011. Hepatoprotective effect of guava (*Psidium guajava* L.) Leaf extracts on ethanol-induced injury on clone 9 rat liver cells. Food Nutr. Sci. 2. https://doi.org/10.4236/fns.2011.29133.

Chon, S.K., Kim, N.S., 2005. Evaluation of silymarin in the treatment on asymptomatic Giardia infections in dogs. Parasitol. Res. 97 (6), 445–451. https://doi.org/10.1007/s00436-005-1462-z.

Das, S., Reiner, D.S., Zenian, J., et al., 1988. Killing of *Giardia lamblia* trophozoites by human intestinal fluid in vitro. J. Infect. Dis. 157 (6), 1257–1260. https://doi.org/10.1093/infdis/ 157.6.1257.

de Araújo, A.A., Soares, L.A.L., Ferreira, M.R.A., de Souza Neto, M.A., da Silva, G.R., de Araújo Jr, R.F., et al., 2014. Quantification of polyphenols and evaluation of antimicrobial, analgesic and anti-inflammatory activities of aqueous and acetone–water extracts of Libidibia ferrea, Parapiptadenia rigida and *Psidium guajava*. J. Ethnopharmacol. 156 (88–96). https://doi.org/10.1016/j.jep.2014.07.031.

De Souza, F., Parker, T., Ali, A., 2014. Exploring the utility of *Psidium guajava* leaf extract as an adequate treatment for *Giardia lamblia*. J. Altern. Complement. Med. 20 (5). https://doi.org/10.1089/acm.2014.5188.abstract.

Diaz, P., Jeong, S.C., Lee, S., Khoo, C., Koyyalamudi, S.R., 2012. Antioxidant and anti-inflammatory activities of selected medicinal plants and fungi containing phenolic and flavonoid compounds. Chin. Med. 7 (1), 26. https://doi.org/10.1186/1749-8546-7-26.

Díaz-de-Cerio, E., Verardo, V., Gómez-Caravaca, A.M., Fernández-Gutiérrez, A., Segura-Carretero, A., 2017. Health effects of *Psidium guajava* L. Leaves: An overview of the last decade. Int. J. Mol. Sci. 24,18 (4), 897. https://doi.org/10.3390/ijms18040897.

Demirci, M., Delibas, N., Altuntas, I., Oktem, F., Yönden, Z., 2003. Serum iron, zinc and copper levels and lipid peroxidation in children with chronic giardiasis. J. Health Popul. Nutr. 21, 72–75.

Dyab, A.K., Yones, D.A., Ibraheim, Z.Z., Hassan, T.M., 2016. Anti-giardial therapeutic potential of dichloromethane extracts of Zingiber officinale and Curcuma longa in vitro and in vivo. Parasitol. Res. 115 (7), 2637–2645. https://doi.org/10.1007/s00436-016-5010-9.

Eissa, M.M., Amer, E.I., 2012. *Giardia lamblia*: a new target for miltefosine. Int. J. Parasitol. 42 (5), 443–452. https://doi.org/10.1016/j.ijpara.2012.02.015.

Elmadawy, R.S., Radwan, M.E., Mahmoud, M.A., 2016. Biochemical and electron microscopic changes induced by giardia in experimentally infected lambs. Int. J. Vet. Sci. Res. 2 (3), 15–21. https://doi.org/10.18488/journal.110/2016.2.3/110.3.15.21.

Fahmy, A.M., Zalat, R.S., Hegab, A.M., Wafy, W.A., 2019. Alterations in oxidative stress activities and trace elements levels on experimental blastocystosis. J. Gastroenterol. Hepatol. Res. 21,8 (6), 3041–3048.

Farnsworth, N.R., 1988. Screening plants for new medicines. In: Wilson, E.O., Peter, M.F., Biodiversity, second ed. National Academies Press (US), Washington (DC), pp. 83-97.

Forrester, S.J., Kikuchi, D.S., Hernandes, M.S., Xu, Q., Griendling, K.K., 2018. Reactive oxygen species in metabolic and inflammatory signaling. Circ. Res. 122 (6), 877–902. https://doi.org/10.1161/CIRCRESAHA.117.311401.

Freire, J., Patto de Abreu, C.M., da Silveira Duarte, S.M., Araújo, B., de Paula, F., Ribeiro Lima, A., 2014. Evaluation of the protective effect of guava fruits and leaves on oxidative stress. Acta Sci. Biol. Sci. 36, 35–40. https://doi.org/10.4025/actascibiolsci.v36i1. 19839.

Gaur, A., Bhatia, A., 2009. Modulation of phosphatase levels in mice liver by genistein treatment against radiation exposure. Pharmacog. Res. 1 (2), 72–79.

Goyal, N., Shukla, G., 2013. Probiotic Lactobacillus rhamnosus GG modulates the mucosal immune response in Giardia intestinalis-infected BALB/c mice. Dig. Dis. Sci. 58 (5), 1218–1225. https://doi.org/10.1007/s10620-012-2503-y.

Grant, G.H., 1987. Amino acids and proteins. In: Tietz, N.W. (Ed.), Fundamentals of Clinical Chemistry. third ed.,. WB Saunders Company, pp. 328–329.

Gutiérrez, R.M.P., Mitchell, S., Solis, R.V., 2008. *Psidium guajava*: a review of its traditional uses, phytochemistry and pharmacology. J. Ethnopharmacol. 117 (1), 1–27. https://doi.org/10.1016/j.jep.2008.01.025.

Halliez, M.C., Buret, A.G., 2013. Extra-intestinal and long-term consequences of Giardia duodenalis infections. World J. Gastroenterol. 19 (47), 8974–8985. https://doi.org/10.3748/wjg.v19.i47.8974.

Hanevik, K., Hausken, T., Morken, M.H., Strand, E.A., Mørch, K., Coll, P., et al., 2007. Persisting symptoms and duodenal inflammation related to Giardia duodenalis infection. J. Infect. 55 (6), 524–530. https://doi.org/10.1016/j.jinf.2007.09.004.

Hayat, M., 2000. Principles and Techniques of Electron Microscopy: Biological Applications. Cambridge University Press, Edinburgh, UK.

Huang, X.J., Choi, Y.K., Im, H.S., Yarimaga, O., Yoon, E., Kim, H.S., 2006. Aspartate Aminotransferase (AST/GOT) and Alanine Aminotransferase (ALT/GPT) Detection Techniques. Sensors 6 (7), 756–782.

Jayakumari, S., Anbu, J., Ravichandiran, V., Anjana, A., Siva Kumar, G., Maharaj, S., 2012. Antiulcerogenic and free radical scavenging activity of flavonoid fraction of *Psidium guajava* Linn leaves. Int. J. Pharm. Sci. 4, 170–174.

Kaneko, K., Suzuki, K., Iwadate-Iwata, E., Kato, I., Uchida, K., Onoue, M., 2013. Evaluation of food-drug interaction of guava leaf tea. Phytother. Res. 27 (2), 299–305. https://doi.org/10.1002/ptr.4724.

Kaushik, N.K., Bagavan, A., Rahuman, A.A., Zahir, A.A., Kamaraj, C., Elango, G., et al., 2015. Evaluation of antiplasmodial activity of medicinal plants from North Indian Buchpora and South Indian Eastern Ghats. Malar. J. 14 (1), 65. https://doi.org/10.1186/s12936-015-0564-z.

Khanna, R., Joshi, K., Kum, K., Malik, A., Vinayak, V., 1990. An ultrastructural analysis of changes in surface architecture of intestinal mucosa following *Giardia lamblia* infection in mice. Gastroenterol. Jpn. 25 (5), 649–658. https://doi.org/10.1007/BF02779368.

Kiran, T.R., Karaman, U., Arici, Y.K., Yildiz, S., 2019. Comparison of malondialdehyde, nitric oxide, adenosine deaminase and glutathione levels in patients with Entamoeba coli, Enterobius vermicularis, Giardia intestinalis, Demodex spp. positive, hydatid cyst and Toxoplasma gondii serum positive. Annal. Med. Res. 26 (7), 1420–1425.

Kolli, V.K., Kanakasabapathy, I., Faith, M., Ramamoorthy, H., Isaac, B., Natarajan, K., Abraham, P., 2013. A preclinical study on the protective effect of melatonin against methotrexate-induced small intestinal damage: effect mediated by attenuation of nitrosative stress, protein tyrosine nitration, and PARP activation. Cancer Chemother Pharmacol. 71 (5), 1209–1218. https://doi.org/10.1007/s00280-013-2115-z.

Lee, W.C., Mahmud, R., Noordin, R., Piaru, S.P., Perumal, S., Ismail, S., 2013. Free radicals scavenging activity, cytotoxicity and anti-parasitic activity of essential oil of *Psidium guajava* L. leaves against Toxoplasma gondii. J. Essent. Oil Bear. Plants 16, 1, 32–38. https://doi.org/10.1080/0972060X.2013.764196.

Leitsch, D., 2015. Drug resistance in the microaerophilic parasite *Giardia lamblia*. Curr. Trop. Med. Rep. 2 (3), 128–135. https://doi.org/10.1007/s40475-015-0051-1.

McCord, J.M., Fridovich, I., 2014. Superoxide dismutases: you've come a long way, baby. Antioxid. Redox Signal. 20 (10), 1548–1549. https://doi.org/10.1089/ars.2013.5547.

Miklasińska-Majdanik, M., Kępa, M., Wojtyczka, R.D., Idzik, D., Wąsik, T.J., 2018. Phenolic compounds diminish antibiotic resistance of Staphylococcus Aureus clinical strains. Int. J. Environ. Res. Public Health 15 (10), 2321. https://doi.org/10.3390/ijerph15102321.

Mohamed, E.A.K., 2012. Hepatoprotective effect of aqueous leaves extract of *Psidium guajava* and Zizyphus spina-christi against paracetamol induced hepatotoxicity in rats. J. Appl. Sci. Res. 8 (5), 2800–2806.

Moreno, M.I.N., Isla, M.I., Sampietro, A.R., Vattuone, M.A., 2000. Comparison of the free radical-scavenging activity of propolis from several regions of Argentina. J. Ethnopharmacol. 71 (1–2), 109–114. https://doi.org/10.1016/S0378-8741(99)00189-0.

Montgomery, H., Dymock, J., 1961. The determination of nitrite in water. Analyst 86, 414–416.

Muda, I., Atik, N., 2018. Profile of liver function in mice after high dose of *Psidium guajava* linn. extract treatment. Biomed. Pharma. J. 11 (3), 1397–1401.

Naseer, S., Hussain, S., Naeem, N., Pervaiz, M., Rahman, M., 2018. The phytochemistry and medicinal value of Psidium guajava (guava). Clin. Phytosci. 4, 32. https://doi.org/10.1186/s40816-018-0093-8.

Nishikimi, M., Rao, N.A., Yagi, K., 1972. Measurement of superoxide dismutase. Biochem. Biophys. Res. Commun. 46, 849–854.

Neiva, V.D.A., Ribeiro, M.N.S., Nascimento, F.R., Maria do Socorro, S.C., Coutinho-Moraes, D.F., do Amaral, F.M., 2014. Plant species used in giardiasis treatment: ethnopharmacology and in vitro evaluation of anti-Giardia activity. Rev. Bras. Farmacogn. 24 (2), 215–224. https://doi.org/10.1016/j.bjp.2014.04.004.

Oda, S.S., 2012. Histopathological and biochemical alterations of metronidazole-induced toxicity in male rats. Global Veterin. 9 (3), 303–310. https://doi.org/10.5829/idosi.gv.2012. 9.3.65175.

Ohkawa, H., Ohishi, N., Yagi, K., 1979. Assay for lipid peroxides in animal tissues by thiobarbituric acid reaction. Anal. Biochem. 95 (2), 351–358. https://doi.org/10.1016/0003-2697(79)90738-3.

Oppong, T.B., Yang, H., Amponsem-Boateng, C., Kyere, E.K.D., Abdulai, T., Duan, G., Opolot, G., 2020. Enteric pathogens associated with gastroenteritis among children under 5 years in sub-Saharan Africa: a systematic review and meta-analysis. Epidemiol Infect. 2, (148). https://doi.org/10.1017/S0950268820000618 e64.

Owen, R.L., Nemanic, P.C., Stevens, D.P., 1979. Ultrastructural observations on giardiasis in a murine model: I. Intestinal distribution, attachment, and relationship to the immune system of Giardia muris. Gastroenterology 76 (4), 757–769. PMID: 422004.

Pavanelli, W.R., Gutierrez, F.R.S., da Silva, J.J.N., Costa, I.C., de Menezes, M.C.N.D., de Abreu Oliveira, F.J., et al., 2010. The effects of nitric oxide on the immune response during giardiasis. Braz. J. Infect. Dis. 14 (6), 606–612.

Pisoschi, A.M., Pop, A., 2015. The role of antioxidants in the chemistry of oxidative stress: A review. Eur. J. Med. Chem. 97, 55–74. https://doi.org/10.1016/j.ejmech.2015.04.040.

Ponce-Macotela, M., Navarro-Alegría, I., Martínez-Gordillo, M.N., Alvarez-Chacón, R., 1994. Efecto antigiardiásico in vitro de 14 extractos de plantas [In vitro effect against Giardia of 14 plant extracts]. Rev. Invest. Clin. 46 (5), 343–347.

Ponce-Macotela, M., Rufino-González, Y., González-Maciel, A., Reynoso-Robles, R., Martínez-Gordillo, M.N., 2006. Oregano (Lippia spp.) kills Giardia intestinalis trophozoites in vitro: antigiardiasic activity and ultrastructural damage. Parasitol. Res. 98 (6), 557–560. https://doi.org/10.1007/s00436-005-0082-y.

Richmond, W., 1973. Preparation and properties of a cholesterol oxidase from Nocardia sp. and its application to the enzymatic assay of total cholesterol in serum. Clin. Chem. 19 (12), 1350–1356. PMID: 4757363.

Rutkowski, R.B., DEBaare, L., 1966. An ultramicro colorimetric method for determination of total and direct serum bilirubin. Clin. Chem. 12 (7), 432–438.

Ryan, U., Hijjawi, N., Feng, Y., Xiao, L., 2019. Giardia: an under-reported foodborne parasite. Int. J. Parasitol. 49 (1), 1–11. https://doi.org/10.1016/j.ijpara.2018.07.003.

Samardžić, S., Arsenijević, J., Božić, D., Milenković, M., Tešević, V., Maksimović, Z., 2018. Antioxidant, anti-inflammatory and gastroprotective activity of Filipendula ulmaria (L.) Maxim. and Filipendula vulgaris Moench. J. Ethnopharmacol. 1,213,132-137. https://doi.org/10.1016/j.jep.2017.11.013.

Savioli, L., Smith, H., Thompson, A., 2006. Giardia and Cryptosporidium join the 'Neglected Diseases Initiative'. Trends Parasitol. 22 (5), 203–208. https://doi.org/10.1016/j.pt.2006.02.015.

Serradell, M.C., Gargantini, P.R., Saura, A., et al., 2018. Cytokines, Antibodies, and Histopathological Profiles during Giardia Infection and Variant-Specific Surface Protein-Based Vaccination. Infect. Immun. 86 (6), e00773–e817. https://doi.org/10.1128/IAI.00773-17.

Shukla, G., Kaur, T., Sehgal, R., Rishi, P., Prabha, V., 2010. Protective potential of L. acidophilus in murine giardiasis. Cent. Eur. J. Med. 5 (4), 456–463. https://doi.org/10.2478/s11536-009-0139-x.

Suganya, T., Fumio, I., Siriporn, O., 2007. Antioxidant active principles isolated from *Psidium guajava* grown in Thailand. Sci. Pharm. 75 (4), 179–193. https://doi.org/10.3797/scipharm.2007.75.179.

Surai, F.P., 2016. Antioxidant Systems in Poultry Biology: Superoxide Dismutase. J. Anim. Res. Nutr 1, 8 https://doi.org/10.21767/2572-5459.100008.

Taga, M.S., Miller, E.E., Pratt, D.E., 1984. Chia seeds as a source of natural lipid antioxidants. J. Am. Oil Chem. Soc. 61 (5), 928–931. https://doi.org/10.1007/BF02542169.

Taha, T.F., Elakkad, H.A., Gendy, A.S.H., Abdelkader, M.A.I., Hussein, S.S., 2019. In vitro bio-medical studies on *Psidium guajava* leaves. Plant Arch. 19 (1), 199–207.

Tella, T., Masola, B., Mukaratirwa, S., 2019. The effect of *Psidium guajava* aqueous leaf extract on liver glycogen enzymes, hormone sensitive lipase and serum lipid profile in diabetic rats. Biomed. Pharmacother. 109, 2441–2446. https://doi.org/10.1016/j.biopha.2018.11.137.

Tende, J., Eze, E., Tende, Y., Onaadepo, O., Shaibu, A., 2013. Anti-ulcerogenic activity of guava (*Psidium guajava*) leaves extract in rats. Ann. Exp. Biol. 1, 6–9.

Tian, H., Chen, B., Wen, J., 2010. Giardiasis, drug resistance, and new target discovery. Infect. Disord. Drug Targets 10 (4), 295–302. https://doi.org/10.2174/187152610791591629.

Todorova, I., Simeonova, G., Kyuchukova, D., Dinev, D., Gadjeva, V., 2005. Reference values of oxidative stress parameters (MDA, SOD, CAT) in dogs and cats. Comp. Clin. Path. 13 (4), 190–194. https://doi.org/10.1007/s00580-005-0547-5.

Tourani, M., Habibzadeh, M., Karkhah, A., Shokri-Shirvani, J., Barari, L., Nouri, H.R., 2018. Association of TNF-α but not IL-1β levels with the presence of Helicobacter pylori infection increased the risk of peptic ulcer development. Cytokine 110, 232–236. https://doi.org/10.1016/j.cyto.2018.01.003.

Yichoy, M., Duarte, T.T., De Chatterjee, A., Mendez, T.L., Aguilera, K.Y., Roy, D., et al., 2011. Lipid metabolism in Giardia: a post-genomic perspective. Parasitology 138 (3), 267–278. https://doi.org/10.1017/S0031182010001277.

You, D., Park, J., Yuk, H., et al., 2011. Antioxidant and tyrosinase inhibitory activities of different parts of guava (*Psidium guajava* L.). Food Sci. Biotechnol. 20, 1095. https://doi.org/10.1007/s10068-011-0148-9.

Zarebavani, M., Dargahi, D., Einollahi, N., Dashti, N., Safari, F., Rezaeian, M., 2017. Significance of nitric oxide level in giardiasis. Clin Lab. 1,63(1),47–52.

Zhou, P., Li, E., Shea-Donohue, T., Singer, S.M., 2007. Tumour necrosis factor alpha contributes to protection against *Giardia lamblia* infection in mice. Parasite Immunol. 29 (7), 367–374. https://doi.org/10.1111/j.1365-3024.2007.00953.x.